J. OF RECEPTOR & SIGNAL TRANSDUCTION RESEARCH, 16(5&6), 339–355 (1996)

THE ROLE OF RECEPTOR KINASE ACTIVITY AND THE NPEY^{960} MOTIF IN INSULIN-ACCELERATED RECEPTOR-MEDIATED INSULIN INTERNALIZATION

Robert M. Smith[1], Shunli Zhang[1], Morris F. White[2] and Leonard Jarett[1*]
[1]Department of Pathology and Laboratory Medicine, University of Pennsylvania Medical Center, Philadelphia, PA 19104 and [2]The Joslin Diabetes Center, Boston, MA 02215

ABSTRACT

This study used biochemical and quantitative ultrastructural approaches to examine the roles that insulin receptor β subunit kinase activity, the NPEY motif in the juxtamembrane region, and tyrosine phosphorylation within that domain plays in insulin-accelerated receptor-mediated insulin internalization in CHO cells. Internalization of insulin in cells that expressed kinase-deficient receptors (CHO_{A1018}) or receptors lacking the NPEY Ala^{954}-Asp^{965} domain ($CHO_{\Delta 960}$) was reduced by 80% compared to cells expressing wild-type human insulin receptors (CHO_{HIRc}). Ultrastructural analysis revealed that the decreased internalization in CHO_{A1018} cells was due to the reduced ability of the kinase deficient receptor to migrate from the microvilli of cultured cells and aggregate on the cell surface. Deletion of the NPEY motif in the juxtamembrane region of the β subunit severely reduced receptor migration, interfered with the normal aggregation of receptors on the cell surface, and virtually eliminated accumulation of the occupied receptors in the coated invaginations. Replacement of Tyr^{960} in the NPEY domain with phenylalanine (CHO_{F960}) had no significant effect on insulin internalization, receptor mobility, aggregation or accumulation in coated invaginations. In contrast, replacement of Tyr^{960} with alanine (CHO_{A960}) decreased insulin internalization, slowed migration, receptor aggregation and accumulation in coated invaginations. These studies document that kinase activity is required, but not sufficient, for receptor movement from the microvilli and aggregation of occupied receptors on the non-villous surface. An intact NPEY motif or surrounding amino acids, but not the phosphorylation of Tyr^{960} plays a role in receptor mobility and aggregation and is essential for the accumulation of insulin receptors in coated invaginations.

INTRODUCTION

The factors regulating the internalization of the insulin receptor and insulin are complex and are not completely understood. Whether or not insulin internalization plays

a role in insulin action is controversial. There is, however, a consensus that an understanding of the molecular and cellular mechanisms regulating insulin internalization is essential to elucidating the potential role of insulin endocytosis in normal tissues and determining whether defects in these processes contribute to the pathophysiology of diabetes and insulin resistance. In this study, we used high resolution electron microscopic techniques to quantitatively examine the initial steps involved in insulin internalization in Chinese hamster ovary cells expressing normal human insulin receptors and compared them to cells expressing receptors with various mutations in the ß subunit. The ultrastructural observations were compared to the biochemically determined effects of these mutations on insulin internalization. The effects of the mutations on insulin-stimulated biological responses have been characterized previously by Backer and colleagues (1–4).

Insulin is internalized by two mechanisms: receptor-mediated and fluid-phase endocytosis (3, 5, 6). The receptor-mediated pathway occurs consitutively, but is also stimulated by insulin binding, so called ligand-accelerated receptor-mediated internalization. Unlike fluid-phase endocytosis, receptor mediated insulin uptake is saturable, with respect to hormone concentration, suggesting it is mediated by a limited number of specific receptors. Fluid-phase endocytosis of molecules is proportional to their extracellular concentration. Rates of fluid-phase endocytosis can vary greatly among different cell types and insulin increases fluid-phase endocytosis of extracellular molecules (7), presumably including insulin.

The duplicity of internalization processes and the complexity of insulin's effects on them in cells expressing normal or mutated receptors contribute to the difficulty of precisely defining the molecular and physiologic mechanisms involved in insulin and insulin receptor internalization, and perhaps some of the disparities in the literature. In the present study we used quantitative high resolution electron microscopy coupled with biochemical analysis to assess the initial events leading to the internalization of occupied insulin receptors in Chinese hamster ovary (CHO) cells expressing wild-type or mutated human insulin receptors. The results of these studies suggest that the movement of insulin receptors from the microvilli to the non-villous surface required a kinase-competent insulin receptor. However, kinase competency alone was not sufficient to achieve normal receptor redistribution. An intact NPEY motif and/or the surrounding amino acids was required for optimal receptor localization to coated invaginations on the

surface of CHO cells and maximal insulin internalization, but receptor localization in coated pits was not dependent on tyrosine phosphorylation of the NPEY motif.

MATERIALS AND METHODS:

Expression Plasmids, Transfection and Culture of CHO Cells

The wild-type insulin receptor expression plasmid pCVSHVIRc as well as expression plasmids encoding mutant human insulin receptors in which alanine replaced Lys^{1018} (IR_{A1018}), phenylalanine or alanine replaced Tyr^{960} (IR_{F960} or IR_{A960}), or a deletion of Ala^{954}-Asp^{965} ($IR_{\Delta 960}$) have been described (8, 9, 4, 1). CHO cells were transfected by calcium phosphate precipitation, selected, and clonal cell lines established as described (1). When the cells were originally received, a large number of flasks were grown of each type and those cells were frozen in liquid nitrogen as the "zero passage stock." Cells used in this study were from passages 2–8. Cells were maintained in culture as described (1) and were harvested just prior to reaching confluence.

[^{125}I]-Insulin Binding, Dissociation, Internalization and Degradation

[^{125}I]-A14-insulin was prepared and purified by reverse phase HPLC as described (10). CHO cells were harvested from the flasks using 0.025% trypsin/1 mM EDTA in PBS which was neutralized after 60 sec with trypsin soy bean inhibitor. The cells were washed three times and resuspended to ~10^7 cells/ml in 128 mM NaCl, 5 mM KCl, 5 mM NaH_2PO_4, 1.5 mM $MgSO_4$, 1.5 mM $CaCl_2$, and 25 mM MOPS (3-[N-morpholino]propanesulfonic acid), pH 7.4, (KRM buffer) with 1% bovine serum albumin. CHO_{Neo} cells were resuspended to 5 x 10^7 cells per ml. Insulin binding, internalization and degradation was determined as described (11) by incubating the cells at various temperatures and times with the [^{125}I]-insulin concentrations as indicated in the legends to the figures. Non-receptor cell associated [^{125}I]-insulin, i.e., non-specific binding or fluid-phase internalization, was estimated in cells incubated with 4.2 μM unlabeled insulin. Insulin dissociation rates were determined by incubating cells for 2 hr at 4°C with 1.7 nM [^{125}I]-insulin to label surface receptors. The cells were washed to remove free insulin by microfuge centrifugation and resuspended to the original volume in buffer and incubated at 37°C in the presence or absence of 1.7 nM unlabeled insulin. Aliquots of the cells were collected by microfuge centrifugation at various time points (2–10 min) and cell associated [^{125}I]-insulin determined as described (11).

Au-Insulin Binding and Internalization

Colloidal gold-labeled insulin (Au-Ins) was prepared, purified and characterized as described (12). CHO cells were incubated with 17 nM Au-Ins at the temperatures and times indicated in the legends to the figures and tables. Non-receptor cell associated Au-Ins, i.e., fluid-phase internalization, was estimated in cells incubated with 4.2 μM unlabeled insulin. To determine the initial distribution of insulin receptors on the cells, aliquots of the cells were prefixed with 4% paraformaldehye in PBS buffer for 30 min at 4°C as described (13). After the prefixation, the cells were washed three times with 50 mM Tris-HCl in PBS to neutralize reactive amino groups and prevent non-specific Au-Ins binding. The prefixed cells were then resuspended in KRM buffer and incubated with Au-Ins for 60 min at 4°C.

Following the incubations the cells were diluted ~10 fold in 2% glutaraldehyde in PBS buffer at 4°C and collected by centrifugation at 500 xg for 5 min. The supernatants were aspirated and fresh fixative added for 60 min. The cell pellets were processed for electron microscopic analysis as described (12). The cells were examined and photographed in a JEOL 100CX electron microscope. The location of Au-Ins particles on a minimum of 100 randomly selected thin sectioned cells was determined for each incubation condition in three separate experiments by viewing the cells directly in the electron microscope. Another investigator took photographs of 25 randomly selected cells. The results obtained in the photographs were compared to the visual observations to insure the objectivity and accuracy of the visually-obtained data. Au-Ins particles were analyzed for their location, e.g., microvilli, non-villous plasma membrane, coated and non-coated invaginations and endosomes, and their aggregation state, e.g., single or grouped particles as previously (13).

RESULTS

[^{125}I]-Insulin Binding, Dissociation, Internalization and Degradation:

The relative number of insulin receptors expressed on the cell surface of the various cell types was determined by incubating cells for up to 120 min at 4°C. Differences were observed in receptor occupancy levels among the cell clones. Specific binding of 1.7 nM [^{125}I]-insulin to the parental CHO_{Neo} clone was barely detectable (~0.3 fm/10^6 cells), whereas CHO_{HIRc} cells bound ~33 fm/10^6 cells. The CHO_{A960}, CHO_{F960},

$CHO_{\Delta 960}$ and CHO_{A1018} clones bound 17–24 fm/10^6 cells. Similar relative differences were found among the cell types at insulin concentrations up to 17 nM (data not shown). These variations were consistent with the different expression levels of the insulin receptors in the cell lines as assessed by Western blotting (data not shown).

Binding and internalization of 17 nM [^{125}I]-insulin was determined at 15 to 120 min at 37°C. Figure 1A shows the total cell associated insulin. All cell types except CHO_{Neo} showed a rapid initial phase of binding during the first 5 min of incubation and steady state conditions were achieved by 15 min. In CHO_{HIRc} cells, total cell associated insulin slowly declined after 15 min due to the relatively higher rate of insulin degradation in these cells (data not shown). Figure 1B shows the absolute amounts of insulin internalized by each cell type. Because of the differences in receptor expression levels, the effects of receptor mutations on insulin internalization would be difficult to assess using these data. The differences in receptor number were compensated for by calculating an internalization index for each cell type by subtracting intracellular insulin from total cell associated, to determine membrane associated insulin, and dividing the intracellular insulin by the membrane associated insulin. As shown in Figure 1C, the internalization indices demonstrate that the $CHO_{\Delta 960}$ and CHO_{A1018} cells had greatly impaired internalization abilities (~20% of CHO_{HIRc} cells). CHO_{A960} cells were less impaired (~40% of CHO_{HIRc} cells). CHO_{Neo} and CHO_{F960} cells internalized receptor-bound insulin to the same extent as the CHO_{HIRc} cells. Similar analyses at 0.7 and 1.7 nM [^{125}I]-insulin yielded virtually identical internalization indices (data not shown).

One can correct for the effects of fluid-phase endocytosis in biochemical studies by subtracting the [^{125}I]-insulin counts internalized by cells incubated in the presence of excess unlabeled insulin from counts associated with cells incubated in the absence of unlabeled insulin. When this calculation was performed, we noted that fluid-phase endocytosis was not the same in all cell types. Fluid-phase endocytosis, i.e., non-saturable [^{125}I]-insulin internalization, was approximately the same in CHO_{HIRc}, CHO_{A960}, CHO_{F960} and $CHO_{\Delta 960}$ but was three fold higher in those cells than in CHO_{Neo} or CHO_{A1018} cells (Figure 2). These results suggested that insulin binding to a large number of kinase-competent insulin receptors increased fluid-phase endocytosis of insulin. These data also demonstrated that fluid-phase endocytosis was time-dependent, but the effects of fluid-phase endocytosis on the ultrastructural analysis Au-Ins internalization were negligible at early time points.

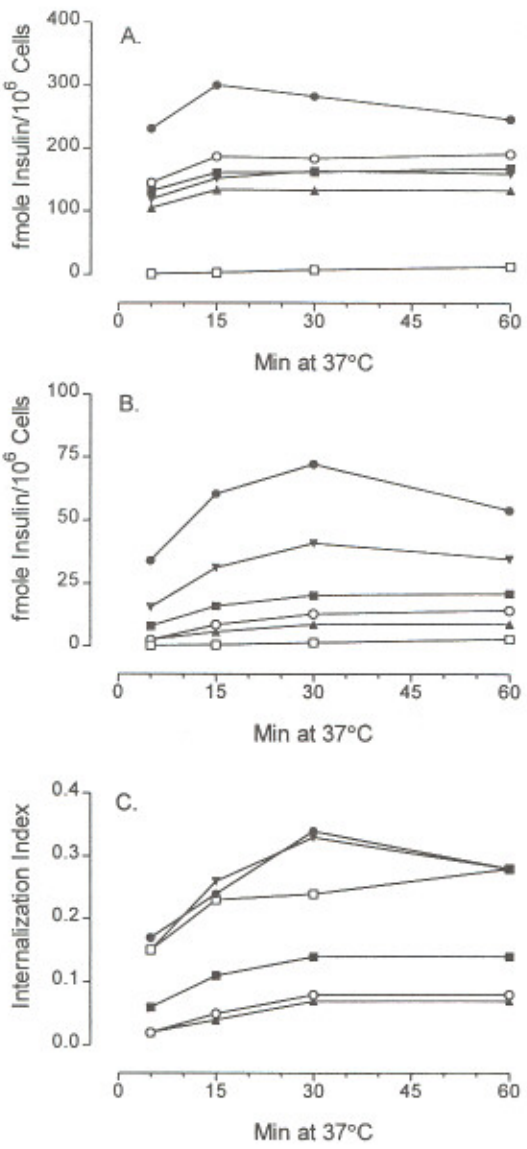

Fig 1: Time Course of [^{125}I]-Insulin Binding and Internalization in CHO Cell Clones. Cells were incubated with 17 nM [^{125}I]-insulin at 37°C for 5–60 min and specific total cell associated (A) and intracellular (B) insulin was determined as described in MATERIALS AND METHODS. An internalization index (C) was calculated as described in MATERIALS AND METHODS to compensate for differences in receptor number among the cell clones. The results are the mean of three determinations; the SD was too small to illustrate. (●) CHO_{HIRc}; (□) CHO_{Neo}; (■) CHO_{A960}; (▼) CHO_{F960}; (▲) $CHO_{\Delta 960}$; (○) CHO_{A1018}.

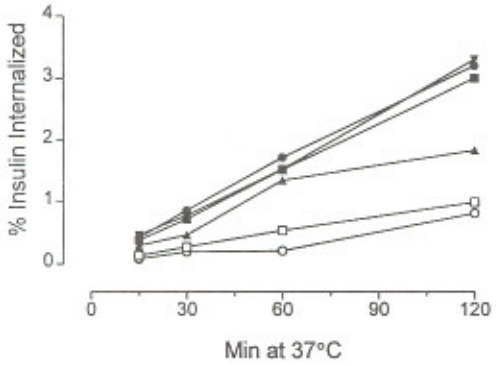

Fig 2: Time Course of Fluid Phase [^{125}I]-Insulin Endocytosis in CHO Cell Clones. Cells were incubated with 17 nM [^{125}I]-insulin in the presence of 4.2 μM unlabeled insulin at 37°C for 5–120 min and intracellular insulin was determined as described in MATERIALS AND METHODS. Insulin internalized in the presence of the unlabeled insulin resulted from non-receptor-mediated internalization, i.e., fluid phase endocytosis. The results are the mean of three determinations; the SD was too small to illustrate. (●) CHO_{HIRc}; (□) CHO_{Neo}; (■) CHO_{A960}; (▼) CHO_{F960}; (▲) $CHO_{\Delta 960}$; (○) CHO_{A1018}.

Because insulin degradation is almost exclusively the result of insulin internalization, insulin degradation was assessed by TCA precipitation analysis in the same experiments. The amount of insulin degraded by each cell type was proportional to the internalization of insulin and was greatly reduced in CHO_{A1018} and $CHO_{\Delta 960}$ cells (data not shown).

In the experiments above, the percent of insulin internalized in CHO_{A960} cells was consistently less than in the CHO_{F960} cells. Insulin dissociation rates were assessed to determine if the site mutations altered this parameter. Figure 3 demonstrates that the initial rate of insulin dissociation from the receptors in CHO_{A960} cells was almost twice that found in the CHO_{HIRc} and CHO_{F960} cells. The reason for this difference is not clear, but it may in part explain the decrease in receptor-mediated insulin internalization in this clone.

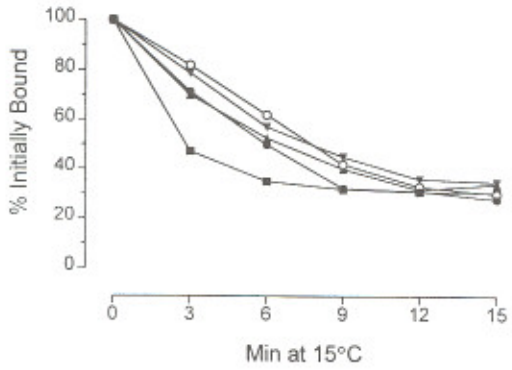

Fig 3: Time Course of Insulin Dissociation From CHO Cell Clones. Cells were incubated with 1.7 nM [^{125}I]-insulin for 2 hr at 4°C, washed to remove unbound insulin and resuspended in buffer containing 1.7 nM unlabeled insulin at 37°C. Cell associated [^{125}I]-insulin was determined at various time points as described in MATERIALS AND METHODS. The results are the mean of three determinations; the SD was too small to illustrate. (●) CHO_{HIRc}; (■) CHO_{A960}; (▼) CHO_{F960}; (▲) $CHO_{\Delta 960}$; (○) CHO_{A1018}.

Au-Insulin Binding and Internalization

Because it is difficult to illustrate the differences in receptor aggregation, mobility, and internalization in "representative" electron micrographs, we performed quantitative analysis of the particle distribution in a minimum of 100 thin sectioned cells from three experiments as described in METHODS AND MATERIALS and those data are presented in the following tables. In all experiments, aliquots of cells were incubated in the presence of 4.2 μM unlabeled insulin which eliminated over 97% of membrane associated Au-Ins under all assay conditions and reduced the intracellular accumulation of Au-Ins to a similar extent for at least 15 min (data not shown).

The ability of the insulin receptors to aggregate is shown in Table 1. No significant differences were found in prefixed cells, which reveals the existing aggregation of unoccupied insulin receptors prior to the addition of insulin. Although cells incubated for up to 2 hr were analyzed, over 90% of the steady-state receptor aggregation occurred within 5 min (data not shown). Insulin-induced receptor aggregation was highest in the CHO_{HIRc} cells. Receptors on CHO_{F960} and CHO_{A960} cells

Table 1

Aggregation of Au-Ins Occupied Receptors

Cell Type	Prefixed	5 min	Δ
		(% of Total Particles)	
CHO_{HIRc}	6.2 ± 1.2	18.7 ± 2.4	12.5
CHO_{A960}	4.4 ± 0.8	10.6 ± 1.8	6.2
CHO_{F960}	6.8 ± 1.2	15.0 ± 2.1	8.2
$CHO_{\Delta 960}$	6.0 ± 1.0	5.7 ± 0.8[(a)]	-0.3
CHO_{A1018}	7.0 ± 1.4	7.4 ± 2.1[(a)]	0.4

[(a)] Significantly different from CHO_{HIRc} cells at $p<0.005$.

Quantitative analysis was performed as described in MATERIALS AND METHODS. Results are the mean ± SD in three experiments.

were 30 and 50%, respectively, as likely to form aggregates than those on CHO_{HIRc} cells. Insulin-induced receptor aggregation was virtually eliminated in CHO_{A1018} and $CHO_{\Delta 960}$ cells. These results suggested that, for perhaps different reasons, kinase deficient receptors and those lacking the NPEY sequence failed to aggregate.

Insulin-stimulated internalization of insulin receptors is believed to require redistribution of the occupied receptors to the non-villous plasma membrane and into endocytic structures. The time-dependent redistribution of insulin receptors was assessed by determining the increase in the percentage of occupied receptors, aggregated or not, on the non-villous plasma membrane as shown in Table 2. The percentage of extracellular particles on the non-villous plasma membrane in prefixed cells was comparable in all cell types except the CHO_{A1018} cells. Redistribution of the receptors on CHO_{HIRc} and CHO_{F960} cells was virtually identical. Approximately 40% of the receptors on these two cell types were on the non-villous plasma membrane within 5 min and there was little further redistribution over a 60 min time course (data not shown). Receptors on CHO_{A960} cells moved more slowly to the non-villous surface but within 15 min reached levels comparable to the CHO_{HIRc} and CHO_{F960} cells. The redistribution of $CHO_{\Delta 960}$ and CHO_{A1018} receptors was greatly reduced and, at steady-stated, was approximately 50% of that seen in the other CHO cells.

Table 2

Redistribution of Au-Ins Occupied Receptors to the Non-Villous Plasma Membrane

Cell Type	Prefixed	5 min	Δ	15 min	Δ
	(% of Total Extracellular Particles)				
CHO_{HIRc}	18.1 ± 3.2	41.6 ± 5.8	23.5	44.8 ± 3.8	26.7
CHO_{A960}	12.3 ± 2.8	29.5 ± 3.8[a]	17.2	38.0 ± 4.2	25.7
CHO_{F960}	14.3 ± 2.3	39.0 ± 3.1	24.7	44.5 ± 2.9	30.2
$CHO_{\Delta 960}$	15.5 ± 2.8	16.7 ± 1.8[a]	1.1	26.5 ± 3.2[a]	11.0
CHO_{A1018}	7.7 ± 2.6[a]	8.5 ± 4.1[a]	0.8	19.4 ± 3.0[a]	11.7

[a] Significantly different from CHO_{HIRc} cells at $p<0.005$.

Quantitative analysis was performed as described in Materials and Methods. Results are the mean ± SD of three experiments.

Our previous studies demonstrated that insulin can be internalized by both non-coated and coated invaginations in many cell types, although cell type-differences may affect the relative amount of insulin internalized by both pathways (14). We determined the number of Au-Ins particles associated with both structures in the CHO cells and expressed the results as a percent of Au-Ins on the non-villous plasma membrane to compensate for the reduced redistribution of the receptors on the $CHO_{\Delta 960}$ and CHO_{A1018} cells.

Approximately 3% of the non-villous Au-Ins particles bound to insulin receptors in prefixed cells that existed in non-coated structures (data not shown). These receptors may represent a portion of the constitutively internalizing pool of receptors on the cell surface. At 5 and 15 min, the percentage of occupied receptors in non-coated invaginations approximately doubled compared to the prefixed cells and there were no significant differences among the cell types (data not shown).

As shown in Table 3, approximately 3% of the non-villous membrane receptors were in coated invaginations in prefixed CHO cells except in $CHO_{\Delta 960}$ cells where receptors were virtually excluded from the coated invaginations. Because the majority of these receptors were single and not aggregated, they may represent another portion of the constitutively internalizing pool of receptors. Except in the $CHO_{\Delta 960}$ cells, the percentage

Table 3

Localization of Au-Ins Particles to Coated Invaginations

Cell Type	Prefixed	5 min	Δ	15 min	Δ
		(% of Non-Villous Membrane Particles)			
CHO_{HIRc}	3.5 ± 0.8	6.9 ± 1.4	3.4	9.2 ± 1.1	5.7
CHO_{A960}	3.2 ± 0.6	5.8 ± 0.9	2.6	8.3 ± 0.9	5.1
CHO_{F960}	3.7 ± 0.8	6.2 ± 0.8	2.5	9.3 ± 1.3	5.6
$CHO_{\Delta 960}$	0.4 ± 0.3[(a)]	1.4 ± 0.8[(a)]	1.0	0.9 ± 0.8[(a)]	0.5
CHO_{A1018}	3.7 ± 0.5	6.7 ± 0.7	3.0	8.7 ± 1.1	5.0

[(a)] significantly different from CHO_{HIRc} cells at $p<0.005$

Quantitative analysis was performed as described in Materials and Methods. Results are the mean ± SD of three experiments.

of receptors in coated invaginations increased by approximately 100% within 5 min and an additional 50% by 15 min. No additional increase was observed through 60 min (data not shown). There was no significant increase in the percentage of $CHO_{\Delta 960}$ receptors in coated invaginations during the first 15 min or through the 60 min time course. Because these data are corrected for the differences in receptor redistribution shown in Table 2, they indicate that receptors lacking the NPEY sequence were excluded from coated invaginations. In contrast, although kinase-deficient receptors on the CHO_{A1018} cells have a substantially reduced ability to move to the non-villous membrane, they were able to move into coated invaginations.

As shown in Table 4, compared to CHO_{HIRc} cells, Au-Ins internalization during the first 15 minutes of incubation was decreased in CHO_{A1018}, $CHO_{\Delta 960}$ and, to a lesser extent, CHO_{A960} cells. However, by 60 min, total intracellular accumulation was nearly the same in all cell types. Between 15 and 60 min the efficacy of unlabeled insulin to block the intracellular accumulation of Au-Ins decreased in a cell-specific and time dependent manner (data not shown). These observations are consistent with fluid-phase endocytosis of Au-Ins. The internalization indices for all cells types based on intracellular Au-Ins in cells incubated for 30 and 60 min in the absence of unlabeled insulin were much greater than the indices for [^{125}I]-insulin at the same time points (data

Table 4

Intracellular Accumulation of Au-Ins Particles

Cell Type	5 min	15 min	60 min
		(% of Total Particles)	
CHO_{HIRc}	23.5 ± 2.2	32.8 ± 3.4	44.7 ± 3.9
CHO_{A960}	16.1 ± 2.8	22.5 ± 2.1	42.5 ± 3.8
CHO_{F960}	22.7 ± 2.4	33.9 ± 3.1	41.7 ± 3.6
$CHO_{\Delta 960}$	12.8 ± 1.8[(a)]	19.3 ± 2.4[(a)]	34.1 ± 2.9
CHO_{A1018}	12.4 ± 1.1[(a)]	17.6 ± 1.4[(a)]	30.9 ± 2.2

[(a)] significantly different from CHO_{HIRc} cells at $p<0.005$

Quantitative analysis was performed as described in Materials and Methods. Results are the mean ± SD of the data acquired in three experiments.

not shown). Intracellular insulin is degraded and iodo-tyrosine is released from the cells. Gold particles are not degraded and continue to accumulate over the time course of the incubation. Reasonably accurate assessments of receptor-mediated internalization of Au-Ins can be made during the first 15 min of incubation, but not at later time points.

DISCUSSION

The objective of these studies was to use quantitative ultrastructural analysis to determine the roles of insulin receptor kinase activity and the NPEY motif in the juxtamembrane region of the receptor ß subunit in insulin-induced receptor internalization. We anticipated that ultrastructural results might provide insights into biochemical analyses of insulin internalization studies performed in these same cells (1–4, 9). Ultrastructural analysis makes it possible to account for the multiple processes involved in insulin internalization, including fluid-phase and constitutive receptor-mediated insulin endocytosis, and definitively analyze effects of these mutations on ligand-induced receptor-mediated endocytosis.

No point mutation or sequence deletion that permits membrane insertion of the insulin receptor has completely obliterated insulin internalization. This, we believe, is due to the multiple mechanisms of insulin internalization. The constitutive internalization of the unoccupied insulin receptors is well documented (15–17). Studies

suggest that a proportion of the insulin receptors are continuously being internalized from the cell membrane and being recycled. Studies in our laboratory have demonstrated significant amounts of insulin were internalized by fluid-phase endocytosis at insulin concentrations greater than 5 nM (6, 11). Similar results (unpublished observations from this laboratory) have been obtained with cells expressing low levels of insulin receptors, e.g., CHO_{Neo}, and 32D myeloid precursor cells (18). Studies by Backer *et* al (3), our laboratory (14), and others (5) have shown that non-saturable or fluid-phase insulin endocytosis is not affected by depletion of intracellular potassium, indicating it is probably not mediated by coated invaginations. The amount of insulin internalized by fluid-phase endocytosis can further hamper analysis of insulin internalization because of insulin's effects on fluid-phase endocytosis (7). As demonstrated in this study, insulin enhanced fluid-phase internalization of insulin in all cells expressing kinase-competent insulin receptors.

Biochemical analyses in this study, which generally confirmed the results of previous studies using these cells (1–4, 9), showed differences in the levels of receptor expression in the five CHO cell clones expressing human insulin receptors. These differences will not affect ultrastructural analysis of insulin-induced receptor aggregation as previously shown (13), but do require some form of equalization, e.g., an internalization index, to compare the cell types. Our results showed that internalization of Au-Ins and [^{125}I]-insulin during the first 5–15 min was decreased by 50–80% in $CHO_{\Delta 960}$ and CHO_{A1018} cells and by 40–60% in CHO_{A960} cells, compared to CHO_{F960} and CHO_{HIRc} cells expressing the wild-type receptor.

Ultrastructural analysis was used to investigate the causes of the decreased internalization. Prefixation of the cells prior to the addition of the Au-Ins demonstrated the constitutive location and aggregation state of the insulin receptors. By comparing receptor location and aggregation in cells incubated for various times with Au-Ins, the effects of ligand-induced receptor mobility, aggregation, and internalization could be determined. There were several significant observations in the prefixed cells. Except in the $CHO_{\Delta 960}$ cells, the distribution of non-villous membrane associated insulin receptors between coated and non-coated invaginations was approximately equal. These receptors may represent receptors in the constitutive internalization pathway. Deletion of the NPEY motif eliminated constitutive localization of insulin receptors in coated

invaginations. This observations suggests that the NPEY sequence, or the sequence of amino acids between Ala^{954}-Asp^{965}, is required for the localization of the insulin receptor to the coated invagination even in the absence of insulin. On prefixed cells, only ~8% of unoccupied kinase-deficient receptors were on the non-villous membrane compared to ~18% for kinase-competent receptors. This suggests that even in the unoccupied state the kinase-deficient receptors was processed differently than normal receptors.

Previous ultrastructural analyses by Carpentier and ourselves have demonstrated that the majority of insulin initially binds to receptors on the microvilli of cultured cells (13, 19, 20) and, after insulin binds, kinase-competent receptors rapidly migrate to the non-villous surface and aggregate whereas, as shown again in this study, mobility of kinase-deficient receptors is severely restricted. Carpentier suggested that insulin binding and activation of the receptor kinase releases a constraint anchoring the receptor to the microvilli (21). Two observations in this study suggest there may be an alternative explanation. First, the kinase-competent receptor expressed in $CHO_{\Delta 960}$ cells failed to migrate from the microvilli. These results demonstrate that activation of the β subunit kinase activity is not sufficient to release an anchoring constraint associated with the receptor on the microvilli. Second, the percentage of kinase-deficient receptors on the non-villous membrane was significantly reduced in prefixed CHO_{A1018} cells. This observation is consistent with the hypothesis that the kinase-deficient insulin receptor is less able to interact with the cellular machinery involved in the constitutive movements of the receptor. While it is not clear how the substitution of Ala^{1018} for Lys^{1018} might have this effect, if this hypothesis is correct, the decreased mobility of insulin-occupied kinase-deficient receptors may not be directly related to insulin's inability to activate the receptor kinase.

Depending on the cell type, insulin can be internalized by both coated and non-coated invaginations. In the present study, accumulation of occupied receptors in non-coated invaginations was not affected by any of the insulin receptor mutations analyzed. Non-coated invaginations most likely represent a constitutive internalization pathway. In contrast, we determined that deletion of 12 amino acids including the $NPEY^{960}$ sequence significantly decreased insulin internalization and had a marked effect on the localization of unoccupied and Au-Ins occupied receptors in coated invaginations. These observations strongly suggest that ligand-accelerated receptor mediated insulin

internalization via coated pits requires the $NPEY^{960}$ motif. Similar sequences, $NPVY^{807}$ and $Y^{20}XRF$, are required or internalization of low density lipoprotein and transferrin receptors, respectively, by coated invaginations. The present biochemical data showed that alanine substitution for Tyr^{960} resulted in decreased insulin internalization whereas the phenylalanine substitution did not. Interestingly, receptors containing either alanine or phenylalanine substitutions effectively localized to coated invaginations when differences in receptor mobility to the non-villous membrane were considered which suggests that Tyr^{960} phosphorylation is not required for localization of the insulin receptor in coated pits. Similar conclusions have been presented previously based on site directed mutagenesis of Tyr^{960} (1, 4, 22). Backer *et al* (4) proposed that the difference between the effects of alanine and phenylalanine substitution on insulin internalization were due to the destabilization of the ß-turn in the juxtamembrane region caused by the former but not the latter, which would prevent the normal association of the IR_{A960} in the coated invagination. We could not confirm that suggestion. We observed an increase in insulin dissociation from receptors with the alanine substitution which we believe contributes to the decrease in receptor mobility, aggregation, and receptor-mediated insulin internalization in the CHO_{A960} cells.

In summary, insulin internalization is a complex process involving fluid-phase, constitutive receptor-mediated, and ligand-accelerated receptor-mediated processes. Fluid-phase endocytosis, although it represents only a small fraction of the internalized insulin at low hormone concentrations, is increased by insulin binding to kinase-competent insulin receptors by an ill-defined mechanism. Endocytosis of insulin on "constitutively" internalizing insulin receptors probably represents a small percentage (10-15%) of the total internalization in normal cells. However, in cells expressing kinase competent receptors insulin may increase the rate of constitutive internalization via the same mechanism(s) by which it affects fluid-phase endocytosis (7). At physiological insulin concentrations the majority of insulin is internalized by a ligand-accelerated receptor-mediated process. Based on observations in this and other studies, a kinase-competent insulin receptor is necessary but not sufficient for the optimal migration, aggregation, and internalization of insulin receptors. Localization in the coated invagination is required for maximal rates of insulin receptor internalization in most cell types and this localization requires the $NPEY^{960}$ and/or surrounding amino acids in the insulin receptor but not the phosphorylation of the tyrosine residues in these motifs.

ACKNOWLEDGEMENTS

This work was supported in part by grants from the NIH: DK28143 (LJ), DK43808 (MFW), and DK19525 (the Diabetes Endocrinology Research Center at the University of Pennsylvania).

REFERENCES

1. Backer JM, Kahn CR, Cahill DA, Ullrich A and White MF. Receptor-mediated internalization of insulin requires a 12-amino acid sequence in the juxtamembrane region of the insulin receptor ß-subunit. J Biol Chem 265, 16450–16454, 1990.

2. Backer JM, Schroeder GG, Cahill DA, Ullrich A, Siddle K and White MF. Cytoplasmic juxtamembrane region of the insulin receptor: a critical role in ATP binding, endogenous substrate phosphorylation, and insulin-stimulated bioeffects in CHO cells. Biochem 30, 6366–6372, 1991.

3. Backer JM, Shoelson SE, Haring E and White MF. Insulin receptors internalize by a rapid, saturable pathway requiring receptor autophosphorylation and an intact juxtamembrane region. J Cell Biol 115, 1535–1545, 1991.

4. Backer JM, Shoelson SE, Weiss MA, Hua QX, Cheatham RB, Haring E, Cahill DC and White MF. The insulin receptor juxtamembrane region contains two independent tyrosine/ß-turn internalization signals. J Cell Biol 118, 831–839, 1992.

5. Moss AL and Ward WF. Multiple pathways for ligand internalization in rat hepatocytes II: Effects of hyperosmolarity and contribution of fluid-phase endocytosis. J Cell Physiol 149, 319–323, 1991.

6. Harada S, Loten EG, Smith RM and Jarett L. Nonreceptor mediated nuclear accumulation of insulin in H35 rat hepatoma cells. J Cell Physiol 153, 607–613, 1992.

7. Gibbs EM, Lienhard GE, Appleman JR, Lane MD and Frost SC. Insulin stimulates fluid-phase endocytosis and exocytosis in 3T3-L1 adipocytes. J Biol Chem 261, 3944–3951, 1986.

8. McClain DA, Maegawa H, Lee J, Dull TJ, Ullrich A and Olefsky JM. A mutant insulin receptor with defective tyrosine kinase displays no biological activity and does not undergo endocytosis. J Biol Chem 262, 14663–14671, 1987.

9. White MF, Livingston JN, Backer JM, Lauris V, Dull TJ, Ullrich A and Kahn CR. Mutation of the insulin receptor at tyrosine 960 inhibits signal transmission but does not affect its tyrosine kinase activity. Cell 54, 641–649, 1988.

10. Harada S, Smith RM, Smith JA and Jarett L. Demonstration of specific insulin binding to cytosolic proteins in H35 hepatoma cells, rat liver and skeletal muscle. Biochem J 306, 21–28, 1995.

11. Smith RM and Jarett L. Partial characterization of mechanisms of insulin accumulation in H35 hepatoma cell nuclei. Diabetes 39, 683–689, 1990.

12. Smith RM, Goldberg RI and Jarett L. Preparation and characterization of a colloidal gold-insulin complex with binding and biological activities identical to native insulin. J Histochem Cytochem 36, 359–365, 1988.

13. Smith RM, Seely BL, Shah N, Olefsky JM and Jarett L. Tyrosine kinase-defective insulin receptors undergo insulin-induced microaggregation but do not concentrate in coated pits. J Biol Chem 266, 17522–17530, 1991.

14. Smith RM and Jarett L. Receptor-mediated endocytosis and intracellular processing of insulin; ultrastructural and biochemical evidence for cell-specific heterogeneity and distinction from non-hormonal ligands. J Lab Invest 58, 613–629, 1988.

15. McClain DA and Olefsky JM. Evidence for two independent pathways of insulin-receptor internalization in hepatocytes and hepatoma cells. Diabetes 37, 805–815, 1988.

16. Smith RM, Gansler TS, Laudenslager NH, Shah N and Jarett L. Heterogeneous effects of inhibitors of receptor processing on insulin binding and intracellular accumulation in various cell types. J Lab Invest 55, 593–597, 1986.

17. Paccaud J-P, Siddle K and Carpentier J-L. Internalization of the human insulin receptor, the insulin-independent pathway. J Biol Chem 267, 13101–13106, 1992.

18. Myers MG, Jr, Grammer TC, Brooks J, Glasheen EM, Wang L-M, Sun XJ, Blenis J, Pierce JH and White MF. The pleckstrin homology domain in insulin receptor substrate-1 sensitizes insulin signaling. J Biol Chem 270, 11715–11718, 1995.

19. Carpentier JL. The journey of the insulin receptor into the cell - from cellular biology to pathophysiology. Histochem. 100, 169–184, 1993.

20. Smith RM, Sasaoka T, Shah S, Takata Y, Kusari J, Olefsky JM and Jarett L. A truncated human insulin receptor missing the COOH-terminal 365 amino acid residues does not undergo insulin-mediated receptor migration or aggregation. Endocrinology 132, 1453–1462, 1993.

21. Carpentier J-L and McClain D. Insulin receptor kinase activation release a constraint maintaining the receptor on microvilli. J Biol Chem 270, 5001–5006, 1995.

22. Kaburagi Y, Momomura K, Yamamoto-Honda R, Tobe K, Tamori Y, Sakura H, Akanuma Y, Yazaki Y and Kadowski T. Site-directed mutagenesis of the juxtamembrane domain of the human insulin receptor. J Biol Chem 268, 126610–16622, 1993.